An Improved Sliding Mode Control for Maximum Power Point Tracking in Photovoltaic Systems

Abdelhakim Belkaid,[1,2,3] Jean-Paul Gaubert,[2]
Ahmed Gherbi [3]

[1]Department of Electromechanics, University of Bordj Bou Arreridj, El-Anasser 34030, Bordj Bou Arreridj, Algeria (Tel: 33-(0)751282309; e-mail: belkaid08@yahoo.fr).
[2]Laboratory of Information Technology and Automatic control for the Systems- LIAS ENSIP, Bat B25, 2 rue Pierre Brousse, BP 633, 86022 Poitiers, France (e-mail: jean.paul.gaubert@univ-poitiers.fr)
[3]Automatic Laboratory of Setif (LAS), University of Setif 1, El Maabouda, Street of Bejaia, 19000 Setif, Algeria (e-mail: gherbi_a@univ-setif.dz)

Abstract: Tracking the maximum power point (MPP) has a great interest in the study of photovoltaic (PV) systems. This task is very difficult due to the non linearity of PV current-voltage characteristics which are dependent on the temperature and irradiation conditions. The sliding mode control (SMC) based MPPT with two different step sizes designed for Boost-type DC/DC converter method is investigated in this paper. The robustness of the proposed controller is tested under rapidly changing solar radiations. The SMC based MPPT is compared to perturb and observe (P&O) method and to incremental conductance (IncCond) method. The PV-MPPT system is simulated by Matlab/Simulink environment and verified by practical implementation within DS1104 R&D controller board. The simulation and experimental results are satisfactory and demonstrate that the new SMC can follow the PV peak power at different operating conditions with best performance.

Keywords: Photovoltaic; dSPACE controller board; Maximum power point tracking; Sliding mode control based MPPT; Boost converter.

1. INTRODUCTION

Direct conversion of the sun's radiation into electrical energy using semiconducting materials is known under the name of photovoltaic effect. Materials presently used for photovoltaic include mono-crystalline silicon, polycrystalline silicon, and amorphous silicon. Unfortunately, these materials exhibit low efficiency in energy conversion. The PV output power generation is influenced by climatic conditions (e.g. irradiance, panel temperature) and load variation.

Therefore a maximum power point tracking (MPPT) technique which is intended to control the DC/DC converter duty cycle is required to ensure an optimal operation of the PV array at different operating conditions (Bratcu, 2008). An overview of more than thirty of these MPPT techniques is done in (Palavee, 2013). Other review articles (Eltawil, 2013; Esram, 2007; Salas, 2006; Subudhi, 2012) give the detailed review of the existing MPPT methods. Among these methods, perturb and observe (P&O) (Femia, 2005; Azzouzi, 2013) and incremental conductance (IncCond) (Dhar, 2013; Safari, 2011) are widely used in the literature, but they fail under fast varying climatic conditions (Ghassami, 2013). The P&O method consists on perturbing the PV output voltage and observing the PV output power to determine the direction of the peak power. The IncCond method tracks the MPP by comparing the instantaneous to the incremental conductance. There are also other techniques such as, fractional short circuit current method (Kollimalla, 2013) which estimates the optimal current by short circuit current and fractional open circuit voltage method (Murtaza, 2012) which estimates the optimal voltage by open circuit voltage. The last two methods are very simple, but they have a weaker and less accurate performance. Reference (Petreus, 2010) compares between four MPPT algorithms which are: fixed step P&O, variable step P&O, incremental conductance and fuzzy logic.

The SMC is mostly used to control the power electronic converters which constitute a case of variable structure systems (Guldemir, 05). Recently, this method is used in photovoltaic systems (Bianconi, 2011; Bianconi, 2013, Komurcugil, 2012) but it is often used to regulate a reference grandeur obtained with another technique such as P&O or IncCond which make the system more complex. This paper proposes SMC based MPPT not to control but to optimize the PV array yield. It is organized as follows, section 2 and 3 provides a modeling of PV array and boost converter, respectively. In section 4, basics of MPPT algorithms are illustrated: P&O, IncCond, and SMC. Thereafter, section 5 and 6 depicts the results of simulations and experiments respectively. Finally, some conclusions are presented in the end of the paper.

2. MATHEMATICAL MODEL OF THE PV ARRAY

Solar cell or PV cell is the elementary component which converts the energy of light directly into electricity by the PV effect. It can produce approximately 2 Watts under 0.5 Volts. Different models based on the PV cell equivalent electrical circuit are used to explain this effect. The one-diode model (Azzouzi, 2013; Ahmad, 2014; Gergaud, 2002; Jamri, 2010) or the two-diode model (Petcut, 2010; Dragomir, 2010) are usually considered. The single diode model (fig. 1) is the

most classical model described in the literature, it includes a current generator to model the incident luminous flux, one diode for the polarization phenomena of the cell, a series resistance representing the various contacts and connections resistances, and a shunt resistance characterizing the various leakage currents due to the diode and to the edge effects of the junction.

Based on experiments, similar models are used also for arrays. Hence, in this paper the mathematical PV array model given by equation (1) (Yu, 2004) will be used.

$$I_{pv} = N_p\, I_{ph} - N_p\, I_s \left[\exp\left(\frac{V_{pv}+\left(\frac{N_s}{N_p}\right)R_s\, I_{pv}}{n_s a\, v_t}\right) - 1\right] - \frac{V_{pv}+\left(\frac{N_s}{N_p}\right)R_s\, I_{pv}}{\left(\frac{N_s}{N_p}\right)R_p} \quad (1)$$

where N_s and N_p are the number of PV panels coupled in series and parallel, respectively; n_s is the number of PV cells connected in series in one branch, I_{pv} is the PV array output current, V_{pv} is the PV array output voltage, R_s and R_p are respectively the PV panel series and parallel resistances, a is the ideality factor.

The photo-current I_{ph} depends on the sunshine G and temperature T as given in the following formula:

$$I_{ph} = [I_{sc}^* + k_i(T - T^*)]\frac{G}{G^*} \quad (2)$$

with k_i is the short circuit current temperature coefficient, $I_{sc}{}^*$ is the short circuit current at standard test conditions (STC) which are solar irradiance G^* of 1000 W/m^2 (1 sun) at spectral distribution of AM 1.5 and cell temperature T^* of 298 Kelvin.

Moreover, the reverse saturation current I_s is calculated using

$$I_s = \frac{I_{sc}^* + k_i(T-T^*)}{\exp\left(\frac{V_{oc}^* + k_v(T-T^*)}{n_s v_t}\right) - 1} \quad (3)$$

where $V_{oc}{}^*$ is the open circuit voltage at STC conditions, k_v is the open circuit voltage temperature coefficient, and $v_t = a\, k_b\, T/q$ is the thermal voltage, $k_b = 1.38065 \cdot 10^{-23}\, J/K$ is the Boltzmann's constant and $q = 1.60218 \cdot 10^{19}\, C$ is the electronic charge.

Fig. 2 depicts the PV module model in SIMULINK environment.

The MSX-60 Solar Panel from Solarex Manufacturer with specifications presented in table I is used for simulations and experiments. Fig. 3 shows the power-voltage and the current-voltage characteristics of the PV module under different irradiation levels with fixed temperature (25°C). These characteristics are achieved using MATLAB simulations with the following parameters $R_s = 0.357\,\Omega$, $R_p = 151\,\Omega$, $n_s = 36$, $a = 1$, $I_{sc}^* = 3.8\,A$, $V_{oc}^* = 21.1\,V$, $k_v = -0.08\,V/°C$, $k_i = 0.003\,\%/°C$.

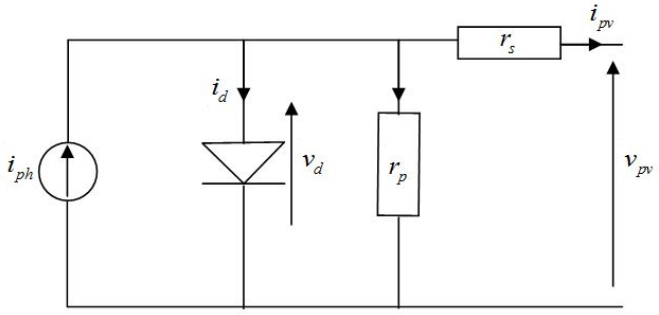

Fig. 1. PV cell electrical model.

From these characteristics, it can be seen that the increase of the irradiation or the decrease in temperature increases the power of the panel.

Figure 4 illustrates the experimental identification of the power-voltage characteristic of three modules coupled in series. The experimental characteristic is obtained by discrete measurement points. These points are achieved successively by varying a resistance load connected directly to the PV source as in (Petcut, 2010). The identifying results coincide totally with the simulation characteristic derived from the mathematical model adopted.

3. MATHEMATICAL MODEL OF THE DC/DC CONVERTER

The studied system consists on solar energy source coupled to adaptation converters (maximum power point trackers, MPPT). These adapters are DC/DC converters with various topologies. The MPPT DC-DC converter delivers power to DC bus and follows the peak power of photovoltaic panel. They accept a DC input voltage and output a DC voltage higher, lower or the same as the input voltage. Most MPPT trackers are based on buck converter (step-down), boost converter (step-up), buck-boost converter or cuk converter.

These converters use inductors and capacitors to control the energy flow from the solar module to the load by continuously opening and closing a switch. The switch is usually an electronic device (MOSFET or IGBT) that operates in two states: in the conduction mode (on) or in the cut-off mode (off). The non-isolated boost dc–dc converters are widely used in stand-alone photovoltaic power systems because of their simplicity and efficiency (Xiao, 2007).

Table 1. MSX 60 solar panel specifications (Ishaque, 2012).

STC Power Rating P_{max}	60 W
Open Circuit Voltage V_{oc}	21.1 V
Short Circuit Current I_{sc}	3.8 A
Voltage at Maximum Power V_{opt}	17.1 V
Current at Maximum Power I_{opt}	3.5 A
Temperature coefficient of V_{oc}	-0.08 V/°C
Temperature coefficient of I_{sc}	0.003 %/°C

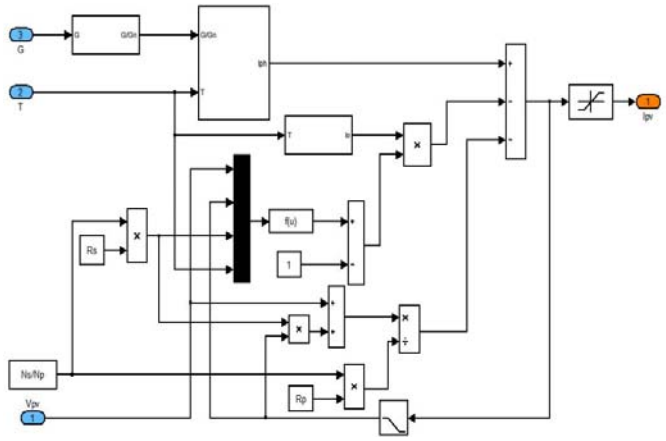

Fig. 2. SIMULINK model of the PV module.

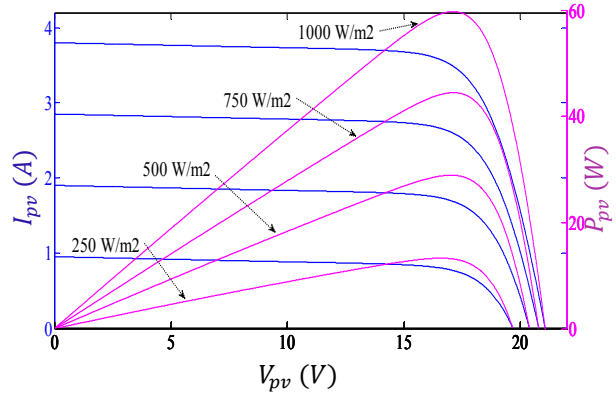

Fig. 3. PV power and current characteristics for different irradiances.

The non-isolated DC/DC boost converter is inserted to interface the PV output to the rest of the conversion chain. This converter is widely used in stand-alone PV power systems, It is characterized by its cyclic ratio d $(0 \leq d \leq 1)$, which helps to express the mean values of the output parameters in function of the input ones. If the chopping frequency is sufficiently high compared to the characteristic frequency of the system, the equations governing the step up type DC-DC converter topology using mean values can be written as follows: (Keshri, 2014)

$$\frac{V_o}{V_{pv}} = \frac{1}{1-d} \tag{4}$$

where V_o is the output capacitor voltage.

In state space form, the dynamic model is obtained as (Radjai, 2014)

$$\begin{cases} \frac{di_L}{dt} = \frac{V_{pv}-V_o}{L} + \frac{V_o}{L} \cdot u \\ \frac{dV_o}{dt} = \left(-\frac{V_o}{RC_2} + \frac{i_L}{C_2}\right) - \frac{i_L}{C_2} \cdot u \end{cases} \tag{5}$$

where i_L is the inductor current. The control input u is the switch position; it is set to 0 when the switch is open and it is set to 1 when the switch is closed.

If we set $x = [x_1 \quad x_2]^{Tr} = [i_L \quad V_o]^{Tr}$ with Tr matrix transpose, then the above expression can be written as:

$$\dot{x} = \frac{dx}{dt} = f(x,t) + g(x,t) \cdot u \tag{6}$$

with $f(x) = \begin{bmatrix} \frac{V_{pv}-x_2}{L} \\ \frac{x_1}{C_2} - \frac{x_2}{RC_2} \end{bmatrix}$, $g(x) = \begin{bmatrix} \frac{x_2}{L} \\ \frac{-x_1}{C_2} \end{bmatrix}$

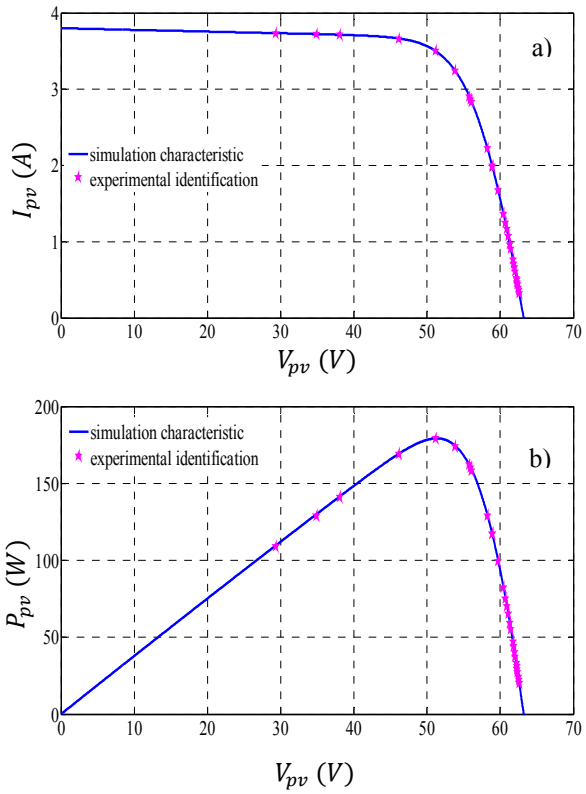

Fig. 4. Experimental identification: a) current-voltage characteristic b) power-voltage characteristic.

4. MPPT TECHNIQUES

4.1 The perturb and observe method

The P&O method is most used in the literature and especially in practice because of its ease of implementation. It works by periodically perturbing (incrementing or decrementing) the panel terminal voltage V_{pv} and comparing the PV output power P_{pv} with that of the previous perturbation cycle. If the perturbation leads to an increase (decrease) in panel power, the succeeding perturbation is made in the same (opposite) direction. In this way, the MPP tracker continuously seeks the peak power condition as described by the algorithm of the Fig.6.

4.2 The Incremental conductance method

The IncCond follows the MPP by comparing the instantaneous conductance (I_{pv}/V_{pv}) with the opposite of incremental conductance $(-dI_{pv}/dV_{pv})$ of the PV array (Radjai, 2014). At the MPP the two items are equal. Fig. 7 gives the flowchart of the IncCond method.

4.3 Improved sliding mode control method

The objective of the sliding mode control is firstly to design switching surface. Then, the second stage consists in conceiving a control law which is responsible to force the

system trajectories towards this area of state space and will maintain it in this one (Bianconi, 2011). On sliding surface, the system has the desired behavior and is insensitive to parameter variations and external disturbances.

As shown in fig. 3, when the PV panel is operating in its MPP, the slope of P-V characteristics is null

$$\frac{dP_{pv}}{dV_{pv}} = \frac{dV_{pv}\, I_{pv}}{dV_{pv}} = I_{pv} + V_{pv}\frac{dI_{pv}}{dV_{pv}} = 0 \tag{7}$$

Then, the switching function can be chosen as the slope of P-V characteristics

$$S = \frac{dP_{pv}}{dV_{pv}} \tag{8}$$

The sliding mode exists on the switching surface $S = 0$. The general control law u combine two terms, a non-linear component u_n, and an equivalent control u_{eq}.

$$u = u_n + u_{eq} \tag{9}$$

u_n to ensure the attractiveness of the control variable to the switching surface; u_{eq} to maintain the operation point in switching surface and displace it to the origin.

These components determined by considering the Lyapunov function L satisfying the control objective both in attractively mode and in sliding mode.

$$L = \frac{1}{2}S(x)^2 \tag{10}$$

To ensure the attractiveness of the control variable to the switching surface, the time derivative of L must be negative definite.

$$\dot{L} = S(x)\cdot\dot{S}(x) < 0 \;\forall\, S(x) \neq 0 \tag{11}$$

The latest expression is known under the name of reaching condition.

From the expression (1), I_{ph} and I_s cannot be established from generally available information. For this, we made some assumptions that are generally valid for silicon cells:

- In an ideal case, the series resistance is neglected and the parallel resistance approaches infinity,
- $\exp\left(\frac{V_{pv}}{n_s a\, v_t}\right) \gg 1$.

By application of the first assumption, the expression (1) becomes:

$$I_{pv} = N_p\, I_{ph} - N_p\, I_s\left[\exp\left(\frac{V_{pv}}{n_s a\, v_t}\right) - 1\right] \tag{12}$$

If the panel is in a short circuit $I_{pv} = N_p\, I_{sc}$ & $V_{pv} = 0$, we can write:

$$I_{ph} = I_{sc} \tag{13}$$

And with second assumption, we can write:

$$I_{pv} = N_p\, I_{sc} - N_p\, I_s \cdot \exp\left(\frac{V_{pv}}{n_s a\, v_t}\right) \tag{14}$$

If the panel is in an open circuit $I_{pv} = 0$ & $V_{pv} = N_s V_{oc}$, we can write:

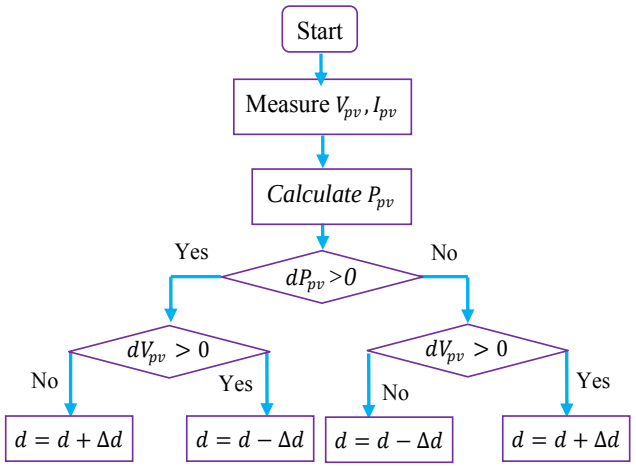

Fig. 6. Flowchart of the perturb and observe method

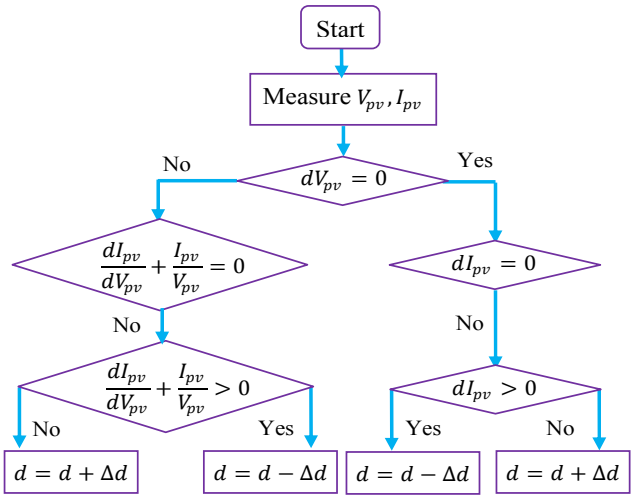

Fig. 7. Flowchart of the Incremental conductance method

$$I_{sc} = I_s \cdot \exp\left(\frac{N_s V_{oc}}{n_s a\, v_t}\right) \Rightarrow I_s = I_{sc} \cdot \exp\left(\frac{-N_s V_{oc}}{n_s a\, v_t}\right) \tag{15}$$

We replace (15) in (14):

$$I_{pv} = N_p\, I_{sc} - N_p\, I_{sc} \cdot \exp\left(\frac{V_{pv} - N_s V_{oc}}{n_s a\, v_t}\right) \tag{16}$$

where V_{oc} is the open circuit voltage, I_{sc} is the short circuit current. And thus,

$$S(x) = I_{pv} + \frac{dI_{pv}}{dV_{pv}} V_{pv} =$$
$$N_p\, I_{sc} - (N_p\, I_{sc} + \frac{N_p\, I_{sc}}{n_s a\, v_t} V_{pv}) \exp\left(\frac{V_{pv} - N_s V_{oc}}{n_s a\, v_t}\right) \tag{17}$$

The derivative is given by:

$$\dot{S}(x) = -(2 + \frac{V_{pv}}{n_s a\, v_t})\frac{N_p I_{sc}}{n_s a\, v_t} \exp\left(\frac{V_{pv} - N_s V_{oc}}{n_s a\, v_t}\right)\frac{dV_{pv}}{dt} \tag{18}$$

When $S(x) > 0$, the system operates on the left of the MPP, the voltage must be increased to attain the MPP ($\frac{dV_{pv}}{dt} > 0$), replacing in (18) it follows that $\dot{S}(x) < 0$, and hence $\dot{S}(x)S(x) < 0$.

When $S(x) < 0$, the system functions in right, the voltage must be decreased ($\frac{dV_{pv}}{dt} < 0$), which implies that $\dot{S}(x) > 0$, therefore $\dot{S}(x)S(x) < 0$.

Thus the system could reach global stability, regardless of the location of the operating point in left or in right of MPP.

To satisfy reaching condition (11), a constant rate reaching law can be selected to the non-linear component

$$u_n = -k_n \cdot sgn(S(x)) \tag{19}$$

where k_n (positive constant), is the scaling factor which is tuned at the design time to adjust the step size.

The equivalent control u_{eq} proposed by Filippov (Slotine, 1991) characterize the system dynamics on the sliding surface, is determined by using the invariance conditions (Komurcugil, 2012):

$$S(x) = 0 \text{ and } \dot{S}(x) = 0 \tag{20}$$

$$\dot{S}(x) = \frac{dS(x)}{dt} = \left[\frac{\partial S}{\partial x}\right]^{Tr} \cdot \dot{x} = \frac{\partial S}{\partial x_1}\dot{x_1} + \frac{\partial S}{\partial x_2}\dot{x_2} \tag{21}$$

From (13), it finds:

$$\frac{\partial S}{\partial x_2} = 0 \;\&\; \frac{\partial S}{\partial x_1} \neq 0 \tag{22}$$

Combination of formulas (20), (21) and (22), implies $\dot{x_1} = 0$, thus, we obtain:

$$u_{eq} = 1 - \frac{V_{pv}}{V_o} \tag{23}$$

After designing the sliding mode via the design of switching function and the reaching mode, it is then possible to express the overall control law by combining (19) and (23)

$$u = 1 - \left(V_{pv}/V_o\right) - k_n \cdot sgn(S) \tag{24}$$

This expression is applied when the operating point moves in the good direction towards the MPP, but if the operating point displaces far from the MPP the parameter k_n must be doubled. From this principle the method takes name of SMC with two different step sizes.

5. SIMULATION RESULTS

This study proposes a novel MPPT method to optimizing the yield of a photovoltaic module. The approach is based on sliding mode control with two different step sizes applied to Boost DC/DC converter as shown in fig. 8.

The work aims to verify the performance of the proposed MPPT tracker. The new method is compared to P&O and IncCond methods. A trapezoidal profile was chosen for varying irradiation between two levels from 500 W/m^2 (maximum power $P_{max} = 30\,W$, optimum voltage $V_{opt} = 8{,}55\,V$, optimum current $I_{opt} = 1{,}75\,A$) to 1000 W/m^2 (maximum power $P_{max} = 60\,W$, optimum voltage $V_{opt} = 17{,}1\,V$, optimum current $I_{opt} = 3{,}5\,A$) for a duration time of 1.2 s . All simulations and experiments tests are made using the switching frequency $\boldsymbol{f = 10kHz}$ and the following parameters: $\boldsymbol{L = 0.5mH}$, $\boldsymbol{C_1 = 1000\mu F}$, $\boldsymbol{C_2 = 470\mu F}$ and $\boldsymbol{T = 298\ Kelvin}$. In simulations, the load is fixed at $\boldsymbol{R = 30\Omega}$.

The obtained simulation results for tracking MPP (maximum power, optimal current, optimal voltage) using P&O, IncCond and SMC are illustrated in fig. 9, fig. 10 and fig. 11, respectively. For example, one can read from fig. 11 at 0.7 second which correspond to standard test conditions (STC) the following values: maximum power $P_{max} = 59.6\,W$, optimum voltage $V_{opt} = 34{,}23 * \left(\frac{1}{2}V\right) = 17.115\,V$, optimum current $I_{opt} = 27{,}8 * \left(\frac{1}{8}A\right) = 3.475\,A$.

Fig. 12 depicts the comparison of tracking MPP between these three methods. It can be noticed that the P&O and the IncCond methods cannot track the true MPP especially when increasing or decreasing the irradiance. Fig. 13 compares the instantaneous efficiency between the new SMC, IncCond and P&O methods. The yield of PV panel by using the proposed algorithm is close to unity from 0.027 s until the end of the irradiance profile. At STC (irradiance of 1000 W/m^2, temperature of 25 °C), the MSX 60 module offers 60 W under optimal voltage value of 17.1 V and optimal current value of 3.5 A.

The results demonstrate that the current of MPP is dramatically affected by fast varying of irradiance, unlike to the MPP voltage which is only slightly affected. Also, it can be seen that the SMC approach has good dynamic response time at start-up; it is ten time faster than the two others methods. From figures of the simulation results, one can conclude that the proposed MPPT method has better performance compared to P&O and IncCond methods during both steady state and dynamic state conditions. In other terms, the proposed MPPT system can track the desired behavior of the maximum power rapidly and with fewer fluctuations which imply good conversion efficiency.

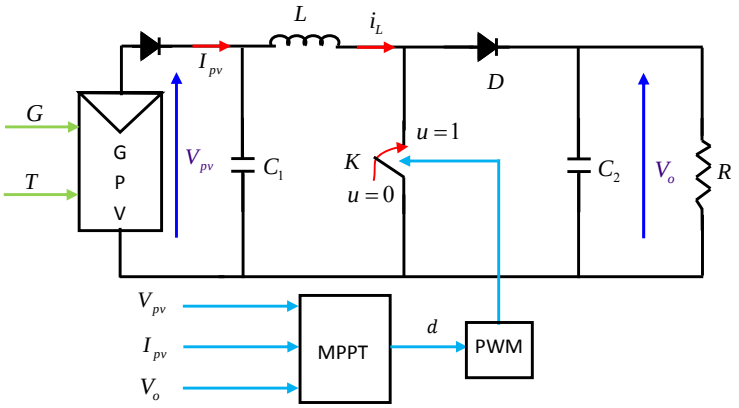

Fig. 8. The proposed MPPT photovoltaic system configuration.

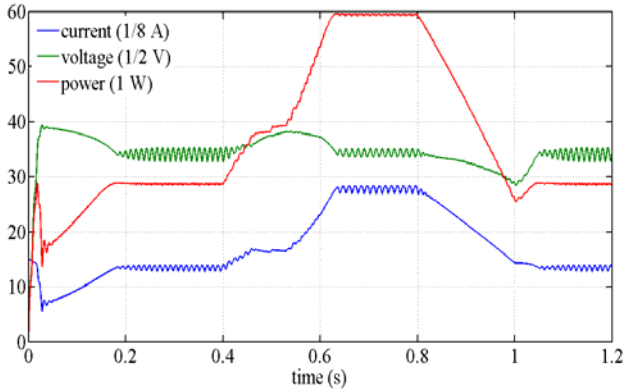

Fig. 9. Tracking MPP by using P&O method.

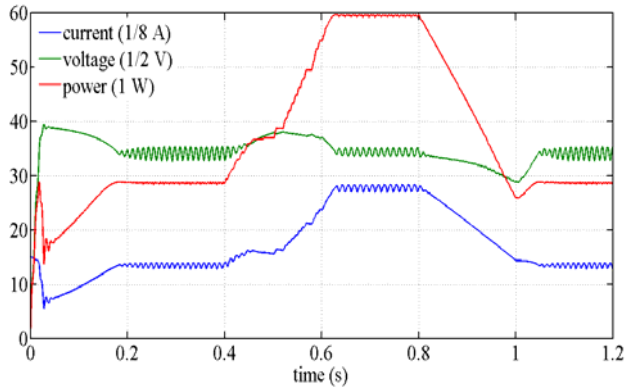

Fig. 10. Tracking MPP by using IncCond method.

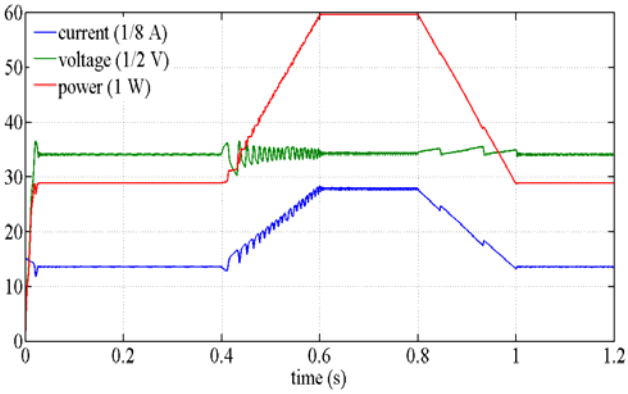

Fig. 11. Tracking MPP by using new SMC method.

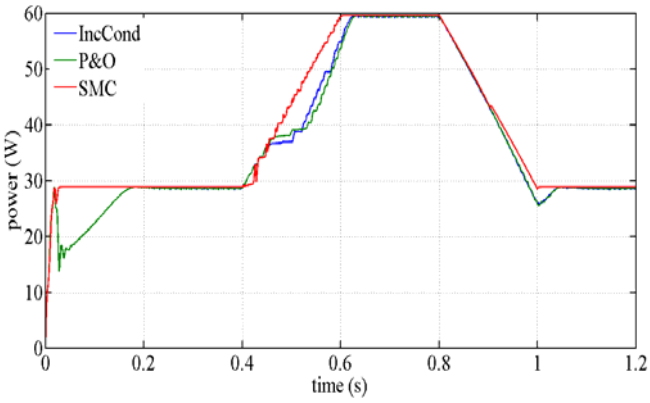

Fig. 12. Tracking MPP for the three methods under a trapezoidal irradiation profile.

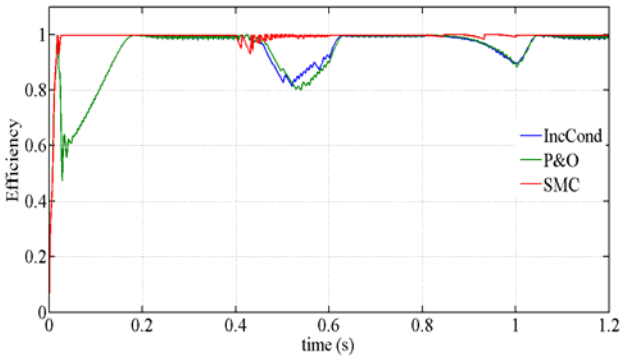

Fig. 13. Comparison of the instantaneous efficiency for the three methods under a trapezoidal irradiation profile.

6. EXPERIMENTAL RESULTS

A test bench has been designed as shown in figure 14. The prototype which was built consists of a TDK-Lambda GEN 300-11 programmable DC voltage source as a photovoltaic emulator, a diode in order to block reverse currents in the PV source, DC/DC boost converter to step up the voltage level and resistance load. The LEM PR30 current probe is used for sensing the PV output current. The differential sensor ST 1000 2-way is used to measure the input and output voltage of the converter. Operational Amplifier is used to amplify the control signals (0-5 V) generated by the dSpace card. Fig. 15 shows clearly the operation of the test bench.

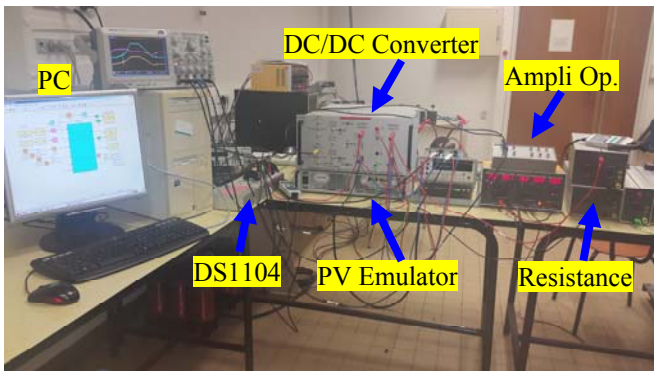

Fig. 14. Experimental test bench.

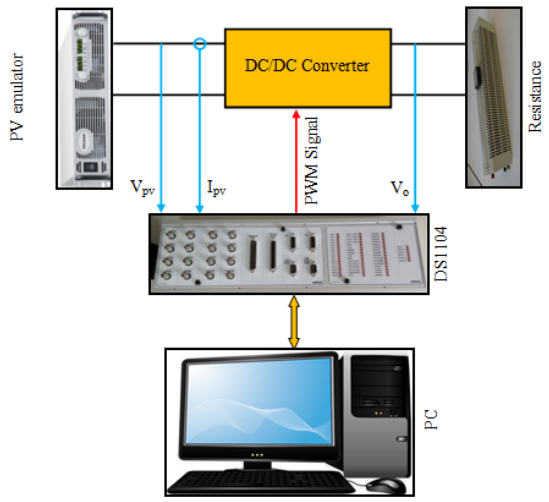

Fig. 15. Implementation of the proposed MPPT algorithm.

Tektronix oscilloscope is used to view the different signals. The MPPT algorithms have been implemented in a DS1104 R&D controller board to generate the PWM signal for acting the IGBT gate of the chopper. Control Desk software is used to supervise the displacement of the MPP on the P-V characteristics under fixed or varying climatic conditions.

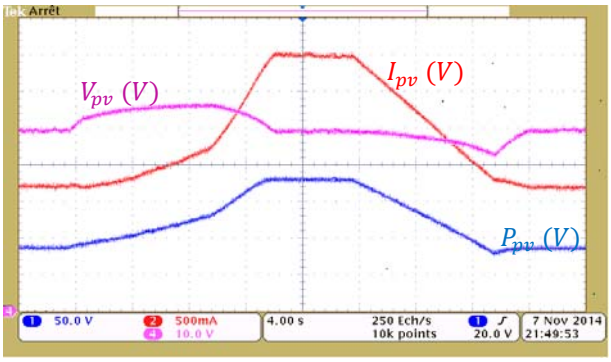

Fig. 16. Experimental measurement of the PV array power, voltage and current using the P&O method.

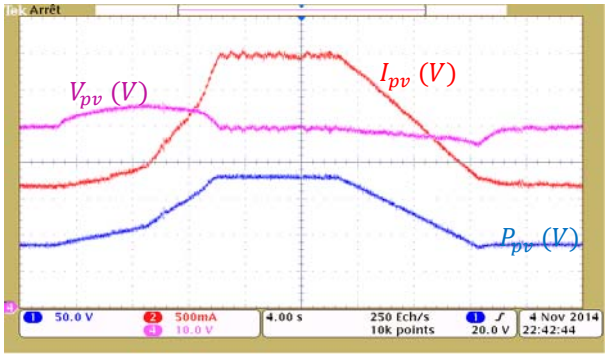

Fig. 17. Experimental measurement of the PV array power, voltage and current using the IncCond method.

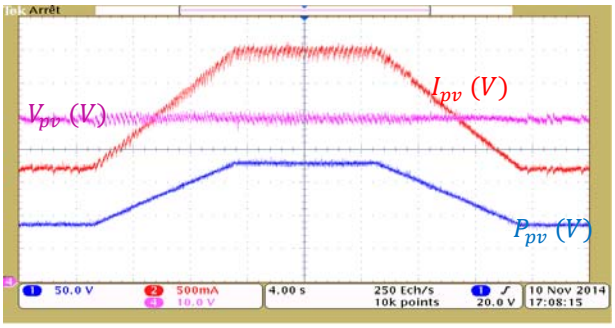

Fig. 18. Experimental measurement of the PV array power, voltage and current using the proposed MPPT method.

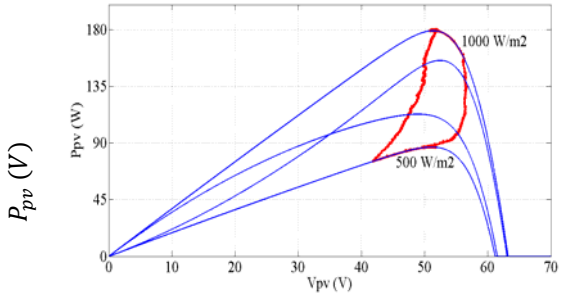

Fig. 19. Tracking the PV peak power using the P&O method

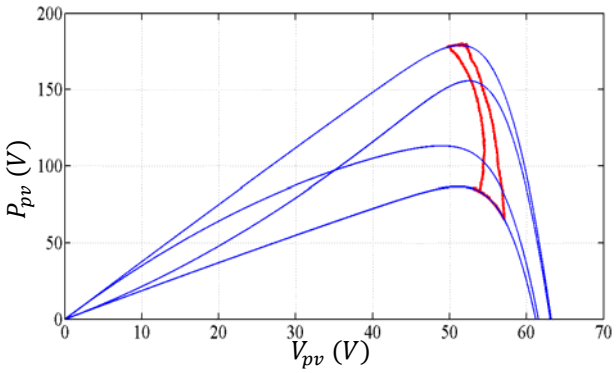

Fig. 20. Tracking the PV peak power using IncCond method

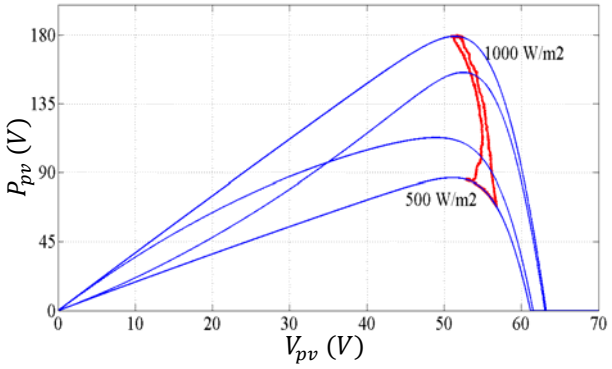

Fig. 21. Tracking the PV peak power using the proposed MPPT method

The PV emulator is programmed for replacing three MSX 60 panels connected serially feeding a resistance of 72 Ω, the temperature is kept fixe at 25 °C and the irradiance is changed with a trapezoidal profile between 500 W/m^2 and 1000 W/m^2. Figures 16, 17 and 18 show the waveforms of output current $\mathbf{I_{pv}(A)}$, voltage $\mathbf{V_{pv}(V)}$ and power $\mathbf{P_{pv}(W)}$ for the P&O, IncCond and SMC respectively. The measurement scale of these grandeurs is as follows: 50 W/div, 500 mA/div, 10 V/div. The results confirm that the optimal current is dramatically affected by rapid-changing irradiance, unlike the optimal voltage which is only slightly affected. In fig. 18 one can see the oscillations in current and voltage curves. These oscillations are acceptable because the ratio of their width to the average value is less than 5%. The experimental results were very similar to the results obtained by simulation. These results either in simulation or in experimental demonstrate that the SMC with two different step sizes is able to track the PV array MPP under constant or rapidly varying of insolation with best performance in both steady and dynamic states compared to P&O and IncCond methods.

Using the Control Desk software, it can be draw Fig. 19, Fig. 20, Fig. 21. These figures present the practical behaviors of tracking MPP during the trapezoidal profile by using P&O, IncCond and improved SMC, respectively. They show the displacement of the peak power (MPP) when the irradiance profile change from 500 W/m^2 to 1000 W/m^2 (rising edge) and from 1000 W/m^2 to 500 W/m^2 (falling edge). The best method is that which takes a more rapid course. From the results, it can be concluded that the proposed MPPT present

better performance in time response or in conversion efficiency than the P&O and IncCond methods.

6. CONCLUSIONS

In this paper, a high performance MPPT based on sliding mode control applied to a boost converter has been presented. The proposed MPPT system by using two different step sizes is capable to track the maximum power under constant and fast changing of solar radiation conditions with best performance in both steady and dynamic states. A compromise between accuracy and rapidity is tacking account when selecting the increments. The new MPP tracker has been compared to P&O and IncCond methods. It is designed, simulated and digitally implemented on the DS1104 R&D controller board**.** So, the aim of this work is attained and it can say that the proposed control technique may be considered as an interesting solution in PV systems control area.

ACKNOWLEDGMENT

The work reported in this paper has been developed within the Laboratory of Information Technology and Automatic control for the Systems (LIAS), Poitiers University, France. And it has been supported by the CNEPRU research project No. J0201220110016, conducted at the department of electrical engineering, University of Setif, Algeria. This support is gratefully acknowledged.

REFERENCES

Ahmad H. Besheer, Ahmed M. Kassem, Almoataz Y. Abdelaziz, (2014). Single-diode model based Photovoltaic module: Analysis and comparison approach, *Electric Power Components and Systems*, 42:12, 1289-1300.

Azzouzi M. (2013). Optimization of Photovoltaic Generator by Using P&O Algorithm under different weather conditions, *CEAI*, Vol.15, No.2 pp. 12-19.

Bianconi E., Calvente J., Giral R., Petrone G., Andres Ramos-Paja C., Spagnuolo G., Vitelli M., (2011),A fast current-based MPPT technique based on sliding mode control, *IEEE International Symposium on Industrial Electronics (ISIE)*, 27-30 June, Gdansk, Poland, 59-64.

Bianconi E., Calvente J., Giral R., Mamarelis E., Petrone G., Andres Ramos-Paja C., Spagnuolo G., Vitelli M., (2013), Perturb and observe MPPT algorithm with a current controller based on the sliding mode, *Electr. Power Energy Syst.* 44, 346-356.

Bratcu A. I., Munteanu I., Bacha S., Raison B., (2008). Maximum Power Point Tracking of Grid-connected Photovoltaic Arrays by Using Extremum Seeking Control, *CEAI*, Vol.10, No.4 pp. 3-12.

Dhar S., Sridhar R., Mathew G., (2013), Implementation of pv cell based standalone solar power system employing incremental conductance mppt algorithm, *IEEE International Conference on Circuits, Power and Computing Technologies (ICCPCT)*, 21st -23rd Mars 2013, Nagercoil, India, pp. 356-361.

Dragomir, T.L. ; Petreus, D.M. ; Petcut, F.M. ; Ciocan, I.C., (2010), Comparative analysis of identification methods of the photovoltaic panel characteristics, *IEEE International Conference on Automation Quality and Testing Robotics (AQTR),1-6*

Eltawil M. A., Zhao Z., (2013), MPPT techniques for photovoltaic applications, *Renewable Sustainable Energy Rev.* 25, 793-813.

Esram, T., Chapman, P.L., (2007), Comparison of photovoltaic array maximum power point tracking techniques, *IEEE Trans. Energy Convers.*, 22, 439–449

Femia N.,Petrone G.,Spagnuolo G.,Vitelli M., (2005), Optimization of perturb and observe maximum power point tracking method. *IEEE Transactions on Power Electronics*; 20 (4): 963–73.

Gergaud B, Multon B, Ben Ahmed H (2002) Analysis and experimental validation of various photovoltaic system models. In: Proceedings of the 7th international *ELECTRIMACS* congress, Montréal, 1-6.

Ghassami A.A., Sadeghzadeh S.M., Soleimani A., (2013), A high performance maximum power point tracker for PV Systems, *Electr. Power Energy Syst.* 53, 237-243.

Guldemir H. (2005), Sliding mode control of DC–DC boost converter, *Journal of Appleid Sciences* 5 (3), 588-592.

Ishaque, K., Salam, Z., Amjad, M., Mekhilef, S., (2012), An improved Particle Swarm Optimization (PSO)-based MPPT for PV with reduced steady-state oscillation. *IEEE Trans. Power Electron*. 27, 3627–3638.

Jamri M. S. and Wei T. C., (2010), Modelling and Control of a Photovoltaic Energy System Using the State-Space Averaging Technique, *American Journal of Applied Sciences* 7 (5): 682-691,

Keshri R., Bertoluzzo M., Buja G., (2014), Integration of a Photovoltaic panel with an electric city car, *Electric Power Components and Systems*, 42:5, 481-495.

Kollimalla S.K., Mishra M.K., (2013), A new adaptive P&O MPPT algorithm based on FSCC method for photovoltaic system, *International Conference on Circuits, Power and Computing Technologies, ICCPCT*, 21st -23rd Mars 2013, Nagercoil, India, 406-411.

Komurcugil H., (2012), Adaptive terminal sliding-mode control strategy for DC–DC buck converters, *ISA Transactions* No.51 (2012), pp.673-681.

Murtaza A.F., Sher H.A., Chiaberge M., Boero D., De Giuseppe M., Addoweesh K.E., (2012), A novel hybrid MPPT technique for solar PV applications using perturb & observe and fractional open circuit voltage techniques, 15th *International Symposium on Mechatronika*, 5th-7th December, Prague, Czech, pp. 1-8.

Pallavee Bhatnagar A. and Nema B. R. K., (2013), Conventional and global maximum power point tracking techniques in photovoltaic applications: A review, *j. renew. sustainable energy* 5, 032701 (2013).

Petcuţ F., Dragomir T.L., (2010), Solar Cell Parameter Identification Using Genetic Algorithms, *CEAI*, vol. 12, No. 1, 30-37

Petreus, D. ; Moga, D. ; Rusu, A. ; Patarau, T. ; Daraban, S., (2010), A Maximum Power Point tracker for photovoltaic system under changing luminosity conditions, 2010 *IEEE International symposium Industrial Electronics (ISIE)*, 556 – 561

Radjai T., Rahmani L., Mekhilef S., Gaubert J-P., (2014), Implementation of a modified incremental conductance

MPPT algorithm with direct control based on a fuzzy duty cycle change estimator using dSPACE, *Solar Energy*, 110 (2014) 325-337.

Safari, A., Mekhilef, S., (2011), Simulation and hardware implementation of incremental conductance MPPT with direct control method using cuk converter, *IEEE Trans. Ind. Electron.*, 2011, 58, pp. 1154–1161

Salas, V., E. Olías, A. Barrado and A. Lázaro, (2006), Review of the maximum power point tracking algorithms for stand-alone photovoltaic systems. *Solar Energy Materials and Solar Cells*, 90, 1555-1578.

Slotine J-J.E., Li W., (1991), *Applied Nonlinear Control*, Prentice-Hall, Englewood Cliffs, New Jersey 07632, p.459.

Subudhi B., Pradhan R., (2012), A comparative study on maximum power point tracking techniques for photovoltaic power systems, *IEEE Trans. Sust. Energy*, 89–98

Xiao Weidong, Ozog Nathan, Dunford William G. (2007), Topology Study of Photovoltaic Interface for Maximum Power Point Tracking, *IEEE transactions on industrial electronics*, vol. 54, no. 3, june 2007, 1696-1704.

Yu G.J., Jung Y.S., Choi J.Y., Kim G.S., (2004), A novel two-mode MPPT control algorithm based on comparative study of existing algorithms, *Sol. Energy* 76 455-463.